Electron Spin Coherence Times in Bulk and Quantum Well Zincblende Semiconductors

Wayne H. Lau, J. T. Olesberg, and Michael E. Flatté

Department of Physics and Astronomy, University of Iowa, Iowa City, IA 52242

Abstract

A theory for longitudinal (T_1) and transverse (T_2) electron spin coherence times in zincblende semiconductor quantum wells is developed based on a non-perturbative nanostructure model solved in a fourteen-band restricted basis set. Quantitative agreement between these calculations and measurements is found for GaAs/AlGaAs, InGaAs/InP, and GaSb/AlSb quantum wells.

The recent observation of long-lived (> 100 ns) spatially extended (> 100 μm) coherent spin states in semiconductors suggests the possibility of manipulating nonequilibrium electron coherence to an unprecedented degree in a solid. [1–3] These spin states interact with light, and thus can be used to generate a host of novel dynamic nonlinear optical and electrical effects. [4] The magnitude and persistence of such effects is governed partly by the spin coherence times T_1 and T_2, describing the decay of longitudinal and transverse spin order, respectively. Ultrafast optical measurements have been performed of both T_1 and T_2, although in different geometries. Pump-probe experiments appear well suited for probing T_1, [5–9] whereas resonant pumping experiments have revealed the behavior of T_2. [2,3]

Accurate quantitative calculations of T_1 and T_2 are essential to improving the understanding of spin coherence in nanostructures. Near room temperature these coherence times are expected to be determined by the D'yakonov-Perel' (DP) mechanism. [10] The precessional DP process is a direct result of the spin splitting of the conduction band, which occurs in zero magnetic field at finite crystal momentum in inversion asymmetric crystals. In nanostructures this inversion asymmetry can arise not only from inversion asymmetry of the bulk constituents, but also from interface effects (in non-common atom systems such as InGaAs/InP) and inversion asymmetry in the compositional profile of the nanostructure. D'yakonov and Kachorovskii (DK) have calculated the effect of bulk inversion asymmetry (BIA) on T_1 in zincblende quantum wells. [11]

Recently, however, 300K electron spin lifetimes were reported in n-doped GaAs/AlGaAs multiple quantum wells (MQWs) that are one order of magnitude longer than those predicted from DK theory [7], and discrepancies were also reported for an InGaAs/InP MQW. [8] The DK theory assumes that $k_\parallel \ll \pi/L$, where L is the thickness of the well, and $k_\parallel$ is the in-plane momentum of the quantum well state k_BT above the band edge. None of the wells considered above (for which the well thicknesses were ~ 80Å) satisfy this condition at room temperature. Thus the DK theory is not only quantitatively incorrect, but the approximations which it relies on are not valid for common well widths.

We present in this letter a quantitative theory of T_1 and T_2 that is accurate for a broad range of materials and structures. We begin by clarifying the relationship between T_1 and T_2. This is followed by calculations of T_1 and T_2 due to the DP mechanism for arbitrary applied field directions, for both bulk and quantum well zincblende materials. Calculations of T_2 are in good agreement with measurements in bulk GaAs [3]. For the quantum wells the calculations of T_1, unlike those of DK theory, are applicable to wells of arbitrary thickness and depth. These calculations are in good agreement with measurements for GaAs/AlGaAs [7], InGaAs/InP [8], and GaSb/AlSb quantum wells [9], whereas DK results disagree by roughly an order of magnitude. We also find that for deep, narrow wells, where DK theory might be expected to apply, the perturbative expression it is based on fails.

The central assumption of the DP mechanism is that the electronic spin system is subject to an effective *time-dependent,* randomly oriented magnetic field $\mathbf{H}$ which changes direction with a time τ that is much shorter than the precession time of either the constant applied field $\mathbf{H_o}$ or the random field. The coherence times depend on the transverse ($H_\perp$) and longitudinal ($H_\parallel$) components of the random field, according to [12]

$$T_1^{-1} \propto (H_\perp^2)\tau, \tag{1}$$

$$T_2^{-1} \propto ([H_\perp^2]/2 + H_\parallel^2)\tau, \tag{2}$$

where the constant of proportionality is the same for Eqs. (1) and (2).

In a crystal with inversion asymmetry and spin-orbit coupling there is a spin splitting described by the Hamiltonian $H = \hbar\mathbf{\Omega}(\mathbf{k})\cdot\sigma/2$, where $\mathbf{\Omega}(\mathbf{k})$ is a *momentum-dependent* effective magnetic field. As the electron is scattered from $\mathbf{k}$ to $\mathbf{k}'$ via ordinary orbital (not spin-dependent) elastic scattering, the effective magnetic field changes direction with time. If the crystal is cubic, then $H_x^2 = H_y^2 = H_z^2$, so $H_\perp^2 = 2H_\parallel^2$ and $T_2 = T_1$. The relationship between T_1 and T_2 differs, however, for quantum wells. For a (001) grown quantum well the fluctuating field along the growth direction z vanishes, and

$$T_1^{-1}(\alpha) = T_1^{-1}(\alpha = 0)(1 + \cos^2\alpha)/2, \tag{3}$$

$$T_2^{-1}(\alpha) = T_1^{-1}(\alpha = 0)(2 + \sin^2\alpha)/4, \tag{4}$$

where α is the direction between $\mathbf{H_o}$ and the growth direction. Thus T_2 ranges from T_1 to $2T_1$ depending on α.

Calculations of $T_1(0)$ (which we will now refer to as T_1) require knowledge of both τ and $\mathbf{\Omega}(\mathbf{k})$. The effective time for field reversal (τ_ℓ) depends on the angular index ℓ of the field component (Ω_ℓ). For example, an $\ell = 1$ component (Ω_1) requires a 180$^\mathrm{o}$ change in the angle of $\mathbf{k}$ to change sign, whereas an $\ell = 3$ component (Ω_3) only requires a 60$^\mathrm{o}$ change, so typically $\tau_3 < \tau_1$. We find

$$\frac{1}{T_1} = \frac{1}{n}\int D(E)f(E)[1 - f(E)]\sum_\ell \tau_\ell(E)\Omega_\ell^2(E)dE, \tag{5}$$

where $f(E)$ is the Fermi occupation function, $D(E)$ is the density of states, n is the electron density, and the scattering rates $\tau_\ell^{-1}(E) = \int_{-1}^{1}\sigma(\theta, E)(1 - P_\ell(\cos\theta))d\cos\theta$ for bulk semiconductors and $\tau_\ell^{-1}(E) = \int_0^{2\pi}\sigma(\theta, E)(1 - \cos[\ell\theta])d\theta$ for (001) quantum wells. For both bulk and quantum wells the functional form of the scattering cross-section $\sigma(\theta, E)$ is taken from standard expressions for ionized impurity (II), neutral impurity (NI — such as arises from quantum well interface roughness), or optical phonon (OP) scattering. The τ_ℓ's differ for different mechanisms (e.g., for a quantum well $\tau_1/\tau_\ell = \ell^2$ for II, $\tau_1/\tau_\ell = \ell$ for OP, and $\tau_1/\tau_\ell = 1$ for NI scattering). The magnitude of $\sigma(\theta, E)$ is obtained from the mobility,

$$\mu = (e/mn)\int D(E)f(E)[1 - f(E)]\tau_1(E)EdE. \tag{6}$$

Time reversal invariance requires $\mathbf{\Omega}(\mathbf{k}) = -\mathbf{\Omega}(-\mathbf{k})$, so $\Omega_\ell = 0$ for even ℓ. We obtain the other Ω_ℓ's from a non-perturbative calculation in a fourteen-band basis. This basis, which is the minimum required to generate spin splitting nonperturbatively, consists of two conduction antibonding s states ($\overline{s}$), six valence (bonding) p states, and six antibonding p states ($\overline{p}$). Such a basis has, for example, been used to analyze spin-splitting in heterostructures [13]. The Hamiltonian is well-known, and can be found in Ref. [14]. The parameters that enter this Hamiltonian include the zone-center energies of the constituent bulk semiconductors and the momentum matrix elements between bands, which are obtained from the conduction band mass, the heavy-hole mass, and the g-factor. Previous calculations of T_1 [10] have been performed using a perturbation theory expression, $\Omega_x(\mathbf{k}) \propto k_x(k_y^2 - k_z^2)$ (the other components related by cubic symmetry). Thus for a bulk semiconductor the dominant term comes from the $\Omega_3^2(E) \propto E^3$ component.

Shown in Fig. 1 are calculated spin coherence times (T_2) for GaAs, InAs, and GaSb assuming II scattering. The agreement with experimental measurements [3] for GaAs at the higher temperatures is quite good, whereas for low temperatures other spin relaxation mechanisms are expected to dominate. The electron densities are 10^{16} cm^{-3} for GaAs, 1.7×10^{16} cm^{-3} for InAs, and 1.49×10^{18} cm^{-3} for GaSb. The difference in slope between GaSb and GaAs occurs because GaSb is degenerate for this density. The tabulated mobilities [15] for InAs and GaSb extend only to 77K, so at lower temperatures $\tau_3(E)$ was assumed to have the same value as at 77K. The smaller T_1 in InAs and GaSb is due partly to the larger conduction spin splitting, which originates from a larger ratio of the spin-orbit coupling Δ to the band gap E_g (see Ref. [16] on perturbative expansions of spin splittings). As the relevant electronic states are near the band edge, perturbative expressions for T_1 for these bulk semiconductors [10] are identical to those obtained from the fourteen-band calculation within numerical accuracy. The agreement between calculated and measured T_2's in Fig. 1 provides strong support for the dominance of the D'yakonov-Perel' mechanism of spin decoherence near room temperature.

Experimental measurements [7] of T_1 in 75Å n-doped GaAs/$Al_{0.4}Ga_{0.6}As$ MQWs at 300K are shown in Fig. 2 (filled circles). The experimental results have been adjusted from Ref. [7], for the authors defined an effective spin flip time for a single spin, $\tau_s = 2T_1$, and plotted their results for τ_s. We note that the implicit analogy to collisional relaxation implied by identifying a time τ_s is problematic, for in a collisional mechanism there is no *a priori* relationship between T_1 and T_2.

The DK calculation (crosses in Fig. 2) is of T_1, so the actual discrepancy (using our values of the confinement energy) is only about a factor of 4 for Ref. [7]. The DK theory for (001) quantum wells begins with the perturbative expressions [17] $\Omega_1^2(E) \propto E(4E_c - E)^2$ and $\Omega_3^2(E) \propto E^3$, where E_c is the confinement energy of the quantum well state. Two approximations are then added: *(i)* the contribution from $\Omega_3(E)$ is ignored, and *(ii)* it is assumed that $\Omega_1^2(E) \propto E$, which is the lowest-order expression. The resulting T_1^{-1} [Eq. (5)] is proportional to the mobility [see Eq. (6)] and does not depend on any other aspects of $\sigma(\theta, E)$.

We calculate $\Omega_\ell^2(E)$ for quantum wells within a full fourteen-band nanostructure model to evaluate these approximations. The electronic structure is obtained by writing the nanostructure electronic states as spatially-dependent linear combinations of the fourteen states in the basis. The full Hamiltonian is projected onto this restricted basis set, which produces a set of fourteen coupled differential equations for the spatially-dependent coefficients of the basis states (generalized envelope functions). These equations are then solved in Fourier space according to the method of Winkler and Rössler. [18] Further details will be presented elsewhere [19]. Figure 3 compares the energy dependence of $\Omega_1^2(E)$ and $\Omega_3^2(E)$ for several structures. The cubic dependence of $\Omega_3^2(E)$ for the three bulk semiconductors is confirmed in Fig. 3(a). Fig. 3(b), however, shows that for quantum wells $\Omega_1^2(E)$ is only linear (short dashed line for the GaAs MQW) for a small energy range (~ 20 meV) above the band edge before it begins to deviate. More energetic states than this certainly contribute to the spin coherence times at room temperature. The energy where $\Omega_1 = 0$ is $\sim 4E_c$, so the wider the well, the lower the energy where $\Omega_1^2(E)$ deviates from linear behavior. $\Omega_3^2(E)$ for these structures is shown in Fig. 3(c), and is comparable in magnitude to $\Omega_1^2(E)$. The open circles in Fig. 2 are those now calculated from Eq. (5) using these $\Omega_\ell^2(E)$'s, assuming optical phonon scattering.

Table I presents calculations and experimental measurements of T_1 for several additional systems. The order of magnitude discrepancy between DK calculations and measurements occurs for these systems as well. Given the uncertainty in experimental mobilities and densities, the agreement with experiment for both NI and OP scattering is good for all systems, and is much better than DK theory. Note that OP and NI scattering calculations in the full theory differ from each other by factors of of up to 2 (due to differences in $\tau_\ell(E)$), whereas all scattering mechanisms produce the same result in DK theory. As expected, for several systems the T_1's are much shorter at higher electron densities, for as the carrier distribution is spread further from zone center the effective magnetic fields increase.

The DK approximation *(i)* can be evaluated by comparing OP_1 to OP and NI_1 to NI, where calculations using all terms up to ℓ are designated OP_ℓ and NI_ℓ. The difference is up to 40%. Approximation *(ii)*, however, produces a discrepancy between the DK result and both NI_1 and OP_1 which can greatly exceed an order of magnitude. As the wells become narrower, even the perturbative expressions for Ω_3 and Ω_1 break down. Figure 3(d) shows $\Omega_1^2(E)$ and $\Omega_3^2(E)$ for a thin-layer InAs/GaSb superlattice, indicating very different behavior from the other structures. Thus in the thin-layer limit the perturbative expression that DK theory is based on fails.

These calculations do not consider other sources of inversion asymmetry, arising from asymmetric wells or interface bonding. These are symmetric wells, so structural inversion asymmetry (SIA) does not play a role. In other structures, such as single-interface heterostructures, SIA may play a more important role [20]. Interface bonding asymmetry (native interface asymmetry, or NIA), which arises in no-common-atom structures, could play a role in systems II, IV, or V. The NIA spin splitting for perfect interfaces (imperfect interfaces reduce the NIA contribution) has been calculated for System II in Ref. [21]. By comparing with Ref. [21] we find the spin splitting is dominated by BIA.

We have presented a non-perturbative nanostructure theory for electron spin relaxation based on a fourteen band model which accounts for the constituent zincblende symmetry. The calculated electron spin lifetimes in III-V semiconductor bulk and quantum well materials are in agreement with experimental measurements, indicating the importance of accurate band structure calculations for zincblende type nanostructures. We note that the fourteen-band nanostructure model should also assist in accurate calculations of spin lifetimes via the Elliot-Yafet mechanism at low temperature.

We would like to acknowledge discussions with D. D. Awschalom, T. F. Boggess, J. M. Byers, J. M. Kikkawa, and A. Smirl. We would also like to thank D. D. Awschalom and J. M. Kikkawa for providing mobility data for the bulk GaAs sample of Ref. [3]. This work was supported in part by the Office of Naval Research through Grant No. N00014-99-1-0379.

REFERENCES

[1] D. Divincenzo, Science **270**, 255 (1995); L. Sham, *ibid*, **277**, 1258 (1997); G. Prinz, *ibid*, **282**, 1660 (1998); *ibid* **283**, 330 (1999).

[2] J. M. Kikkawa, I. O. Smorchkova, N. Samarth, and D. D. Awschalom, Science **277**, 1284 (1997).

[3] J. M. Kikkawa and D. D. Awschalom, Phys. Rev. Lett. **80**, 4313 (1998).

[4] E. Knill and R. Laflamme, Phys. Rev. Lett. **81**, 5672 (1999); J. Preskill, Phys. Today **52**, 24 (1999); J. M. Kikkawa and D. D. Awschalom, Science **287**, 473 (2000).

[5] J. Wagner, *et al.*, Phys. Rev. B **47**, 4786 (1993).

[6] R. S. Britton, *et al.*, Appl. Phys. Lett. **73**, 2140 (1998); J. T. Hyland, *et al.*, Semicond. Sci. Technol. **14**, 215 (1999).

[7] R. Terauchi, Y. Ohno, T. Adachi, A. Sato, F. Matsukura, A. Tackeuchi, and H. Ohno, Jpn. J. Appl. Phys. **38**, Pt. 1, No. 4B., 2549 (1999).

[8] A. Tackeuchi, O. Wada, and Y. Nishikawa, Appl. Phys. Lett. **70**, 1131 (1997); R. Tackeuchi, T. Kuroda, S. Muto, Y. Nishikawa, and O. Wada, Jpn. J. Appl. Phys. **38**, Pt. 1, No. 8, 4680 (1999).

[9] K. C. Hall, *et al.*, Appl. Phys. Lett. **75**, 3665 (1999); **75**, 4156 (1999).

[10] M. I. D'yakonov and V. I. Perel', Sov. Phys. JETP **33**, 1053 (1971); Sov. Phys. Solid State **13**, 3023 (1972); *Optical Orientation, Modern Problems in Condensed Matter Science*, edited by F. Meier and B. P. Zachachrenya (North-Holland, Amsterdam, 1984), Vol. 8.

[11] M. I. D'yakonov and V. Yu. Kachorovskii, Sov. Phys. Semicond **20**, 110 (1986).

[12] Y. Yafet in *Solid State Physics Vol. 14*, (Academic Press, New York, 1963), p. 1.

[13] L. Wissinger, *et al.*, Phys. Rev. B **58**, 15375 (1998).

[14] P. Y. Yu and M. Cardona, *Fundamentals of semiconductors, Physics and materials properties*, 2nd ed. (Springer, New York 1999); M. E. Flatté, P. M. Young, L. H. Peng, and H. Ehrenreich, Phys. Rev B **53**, 1963 (1996).

[15] O. Madelung, *Semiconductors-Basic Data*, 2nd ed. (Springer, New York, 1996).

[16] M. Cardona, N. E. Christensen, and G. Fasol, Phys. Rev B **38**, 1806 (1988).

[17] E. L. Ivchenko and G. E. Pikus, *Superlattices and Other Heterostructures*, 2nd ed. (Springer, New York, 1997).

[18] R. Winkler and U. Rossler, Phys. Rev. B **48**, 8918 (1993).

[19] J. T. Olesberg, Ph. D. thesis, University of Iowa, 1999; W. H. Lau, J. T. Olesberg, and M. E. Flatté, to be published.

[20] P. Pfeffer and W. Zawadzki, Phys. Rev. B **52**, R14332 (1995); P. Pfeffer, *ibid* **55**, R7359 (1997); P. Pfeffer and W. Zawadzki, *ibid* **59**, R5312 (1999).

[21] L. Vervoort, R. Ferreira, and P. Voisin, Semicond. Sci. Technol. **14**, 227 (1999).

TABLES

TABLE I. Spin coherence times T_1 (ps) for several structures, I: a 75Å GaAs/$Al_{0.4}Ga_{0.6}As$ MQW [7], II: a 70Å $In_{0.53}Ga_{0.47}As$/97Å InP MQW [8], III: an 80Å GaSb/80Å AlSb MQW [9], IV: a 51Å $GaAs_{0.19}Sb_{0.81}$/80Å AlSb MQW [9], and V: a 21.2Å InAs/36.6Å GaSb superlattice. Calculated times are shown for a given total electron density (n.d. indicates nondegenerate) using DK theory (DK), and the nonperturbative theory with optical phonon (OP) and neutral impurity (NI) scattering. The subscript ℓ indicates that only terms up to Ω_ℓ were used in the calculation.

	Density (cm^{-3})	μ (cm^2/Vs)	Exp.	DK	OP$_1$	OP	NI$_1$	NI
I	2.7×10^{17}	800	100	27	151	120	162	111
II	n.d.	6700	—	1.45	53	37	52	32
	3.0×10^{18}	6700	2.6	0.21	6.0	4.9	6.9	4.0
III	n.d.	2000	—	0.59	1.9	1.8	1.5	1.4
	2.8×10^{18}	2000	0.52	0.09	0.64	0.55	0.88	0.53
IV	n.d.	2000	—	0.09	0.53	0.52	0.44	0.43
	3.4×10^{18}	2000	0.42	0.01	1.9	1.4	1.7	0.87
V	n.d.	3000	—	0.38	0.77	0.77	1.7	1.6

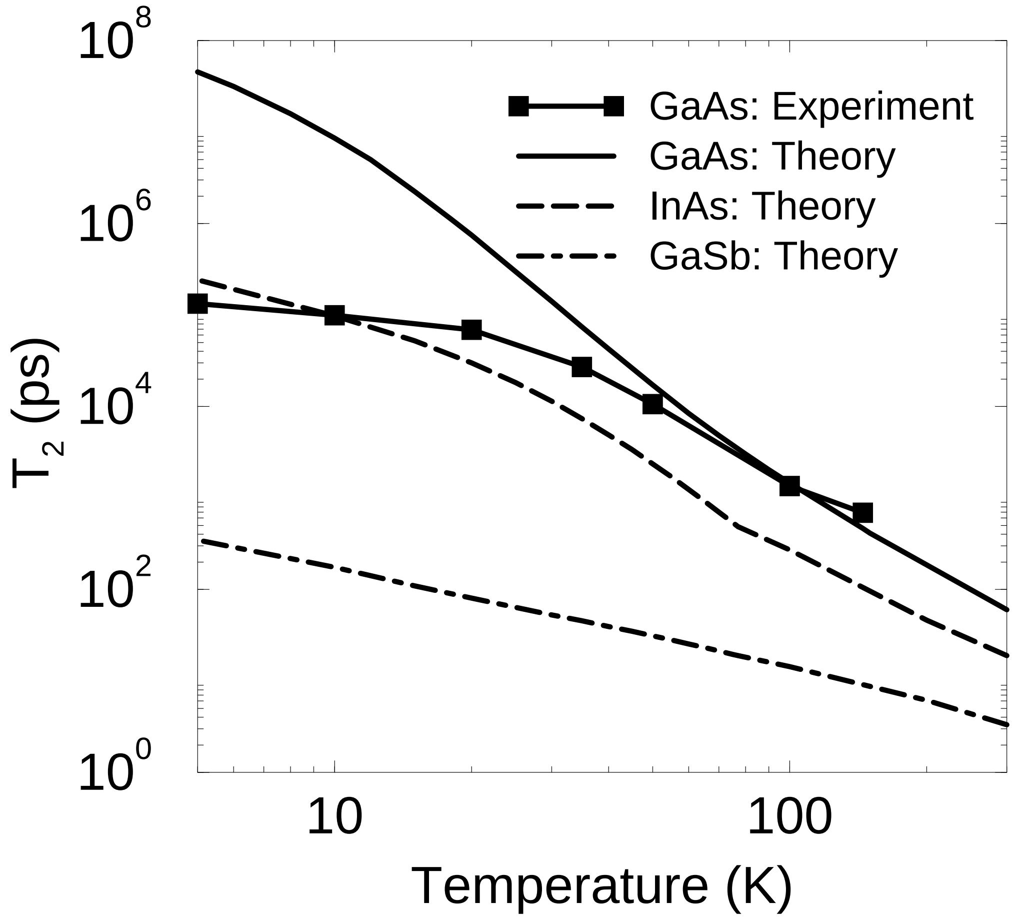

FIG. 1. T_2 in bulk III-V semiconductors as a function of temperature. Solid with squares and solid lines respectively represent the results of experiments [3] and the non-perturbative theory for bulk GaAs at the electron density $n = 1.0 \times 10^{16}$ cm^{-3}. Also shown are results for bulk InAs at $n = 1.7 \times 10^{16}$ cm^{-3} and bulk GaSb at $n = 1.49 \times 10^{18}$ cm^{-3}, which are indicated with dashed and dot-dashed lines respectively.

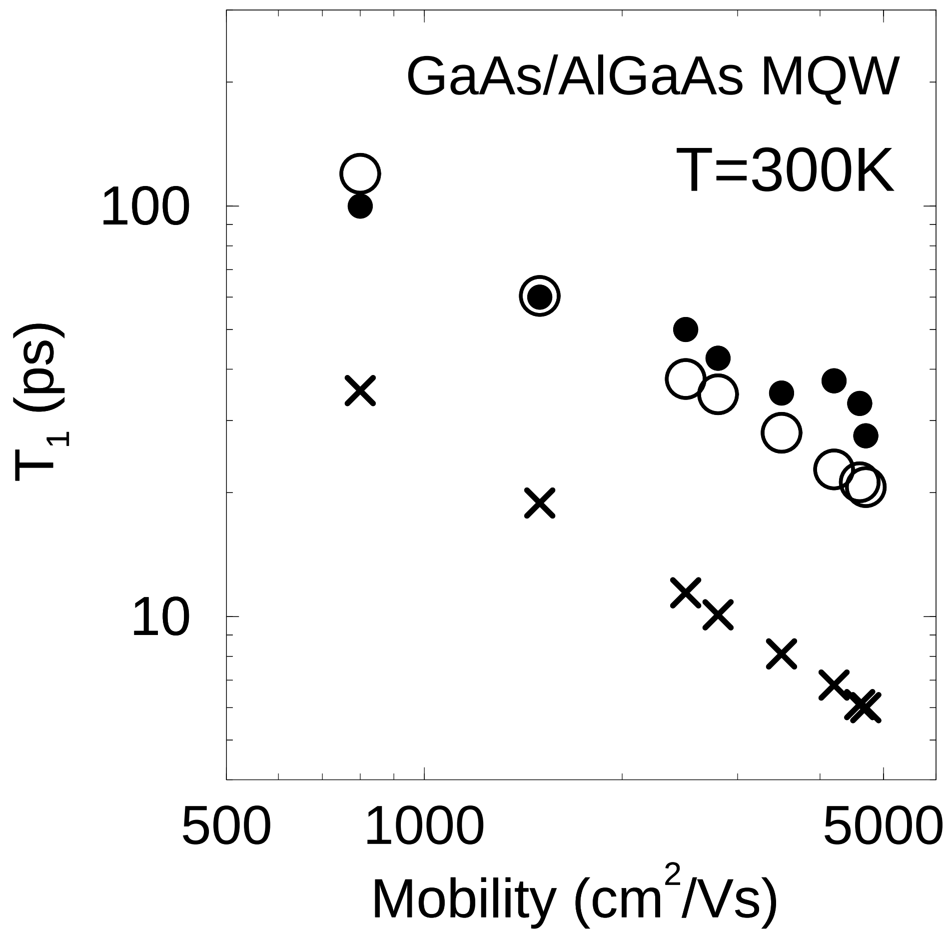

FIG. 2. T_1 as a function of mobility for 75Å GaAs/$Al_{0.4}Ga_{0.6}$As MQWs at room temperature. Closed and open circles respectively represent the results of experiments [7] and the non-perturbative theory, whereas crosses represent the DK theory values. Each experimental point corresponds to a different sample.

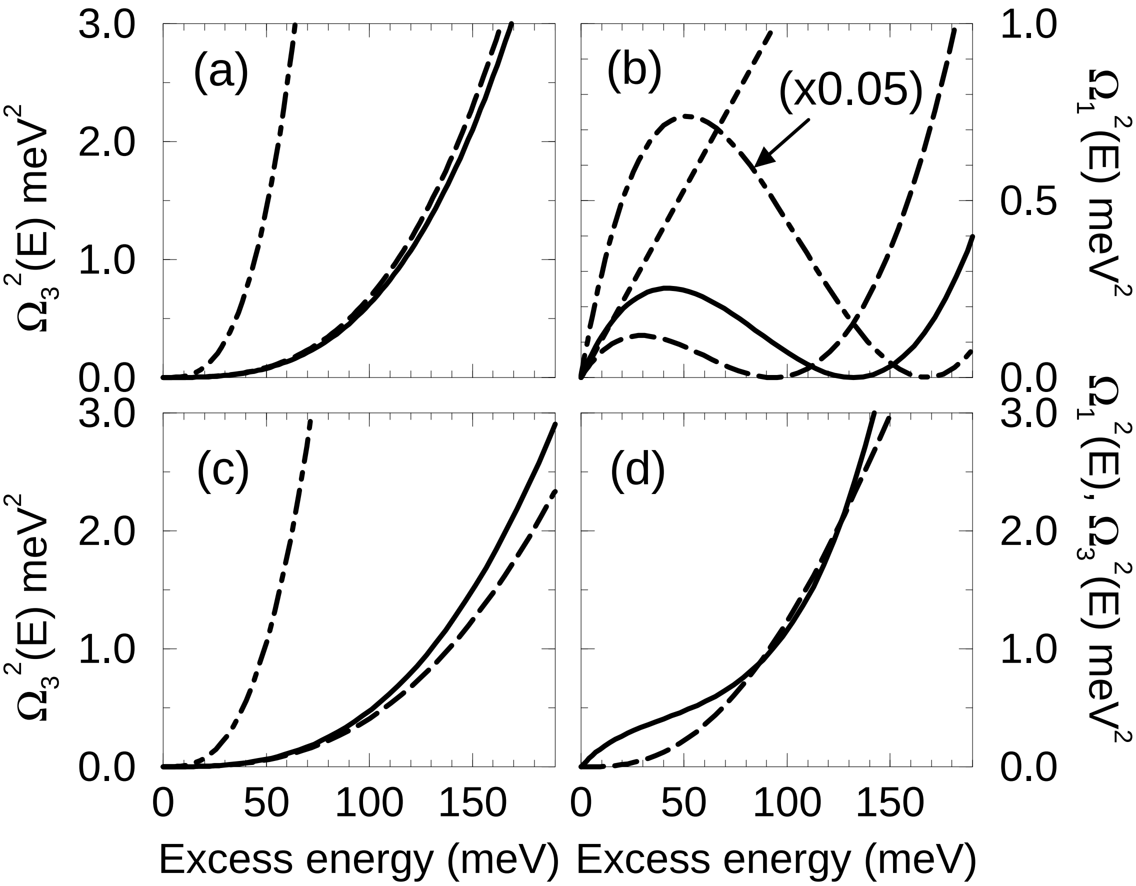

FIG. 3. $\Omega_1^2(E)$ and $\Omega_3^2(E)$ for several structures. (a) $\Omega_3^2(E)$ for bulk GaAs (solid), InAs (dashed), and GaSb (dot-dashed). (b) $\Omega_1^2(E)$ for GaAs (solid), InGaAs (long dashed), and GaSb (dot-dashed) quantum wells described in Table I. The short-dashed line is the DK approximation. (c) $\Omega_3^2(E)$ for the same three structures as (b). (d) $\Omega_1^2(E)$ (solid) and $\Omega_3^2(E)$ (dashed) for a thin-layer InAs/GaSb superlattice.